

# Soft Matter

Accepted Manuscript



This is an *Accepted Manuscript*, which has been through the Royal Society of Chemistry peer review process and has been accepted for publication.

*Accepted Manuscripts* are published online shortly after acceptance, before technical editing, formatting and proof reading. Using this free service, authors can make their results available to the community, in citable form, before we publish the edited article. We will replace this *Accepted Manuscript* with the edited and formatted *Advance Article* as soon as it is available.

You can find more information about *Accepted Manuscripts* in the [Information for Authors](#).

Please note that technical editing may introduce minor changes to the text and/or graphics, which may alter content. The journal's standard [Terms & Conditions](#) and the [Ethical guidelines](#) still apply. In no event shall the Royal Society of Chemistry be held responsible for any errors or omissions in this *Accepted Manuscript* or any consequences arising from the use of any information it contains.

Submitted to *Soft Matter*

**Effects of Terminal Chain Length in Hydrogen-Bonded Chiral  
Switches on Phototunable Behavior of Chiral Nematic Liquid  
Crystals: Helicity Inversion and Phase Transition**

Dengwei Fu, Juntao Li, Jie Wei, Jinbao Guo\*

*College of Materials Science and Engineering, Beijing University of Chemical  
Technology, Beijing 100029, P. R. China.*

\*Correspondence author. Email: [guojb@mail.buct.edu.cn](mailto:guojb@mail.buct.edu.cn),

**Abstract:** A novel series of photoresponsive chiral switches are fabricated by a facile Hydrogen-bonded (H-bonded) assembly method, in which binaphthyl azobenzene molecule is used as the proton acceptor, and binaphthyl acids with opposite chiral configuration are proton donors. We find that the helical twisted power of H-bonded chiral switches and the helical handedness of induced chiral nematic liquid crystals (N\*-LCs) are mainly determined by the terminal flexible chain length in proton donors of binaphthyl acids. Controlling the lengths of the terminal flexible chain leads to different photoswitching behaviors by light irradiation, such as a helical inversion in the N\*-LCs and a phase transition from N\*-LCs to nematic LCs. This is mainly because of chiral counteraction and intensity attenuation of opposite chiral configurations between proton acceptor and proton donor during UV/Vis irradiation. Additionally, thermal switching behavior of N\*-LCs doped with H-bonded chiral switches is also demonstrated, and the related tuning mechanism may be attributed to the H-bonded effect and the changes in a dihedral angle of the binaphthyl rings. This facile assembly approach provides a new way to fabricate functional chiral switches for photonic applications.

## Introduction

Dynamic switching of the chirality in liquid crystals (LCs) has gained much attention due to their potential applications LCs displays, optical sensor, and asymmetric synthesis of organic molecules and polymers.<sup>1-12</sup> Among applied external stimuli such as temperature, electrical or optical field, dynamic controlling by light has attracted great interest due to the fast response time, ease of addressability, and the potential for remote control.<sup>5</sup> An optically tunable helical superstructure can be achieved by doping chiral azobenzene molecules into a nematic LCs (N-LCs) host and the resulting chiral nematic LCs (N\*-LCs) can be efficiently modulated by *trans-cis* photoisomerization of azobenzene dopant. As is well known that, N\*-LCs have the unique property of selective reflection of circularly polarized light (CPL) and the corresponding Bragg reflection wavelengths of N\*-LCs are sensitive to external factors including heat, light irradiation, electric field and so on.<sup>13-20</sup>

Although optically tunable N\*-LCs by controlling helical twisted power (HTP) of chiral dopants has been extensively investigated, there are only a few on the study of the photoresponsive chiral dopants which could induce helix inversion in a N\*-LCs upon UV/Vis light.<sup>21-26</sup> Nevertheless, this kind of material that is associated with CPL reflection has great potentials for smart stimuli-responsive photonic materials.<sup>27-32</sup> Akagi *et al* present dynamic photoswitching of the helical inversion in N\*-LCs based on a series of photoresponsive chiral dithienylethene derivatives bearing two axially chiral binaphthyl moieties, and they found that the N\*-LCs by doping into the chiral dopant featuring the shortest alkyl chain in binaphthyl moiety exhibited the reversible

behavior in helical inversion. However, this special photoswitching behavior depends on a specific LC host, which may limit their practical applications.<sup>24</sup> Li *et al* reported a reversible handedness inversion of a self-organized helical superstructure by employing photoisomerizable chiral cyclic dopants.<sup>25</sup> However, an obvious disadvantage of this system is that the helix inversions induced by light in N\*-LCs mainly rely on chance. Very recently, Li *et al* developed a type of azobenzene compounds with axially chiral binaphthyl units of the opposite chiral configurations. The handedness inversion in different LC hosts could be induced upon light irradiation, and the related switching mechanism is due to the chiral conflict and equilibrium shifting between multiple chiral moieties in a single chiral switch.<sup>26</sup> However, practical realization of such tunable helix inversion in N\*-LCs still suffers from some limitations, such as specific LC host and complicated synthetic process.<sup>21-26</sup>

In this study, we develop a novel series of novel photoresponsive chiral switches by a facile hydrogen-bonded (H-bonded) assembly method. It is well known that, H-bond assembly as a simple but effective way for achieving supramolecular structure has attracted much attention due to their potentials for LC stimuli-responsive materials.<sup>33-35</sup> Here the binaphthyl azobenzene molecule is used as the proton acceptor and binaphthyl acids with opposite chiral configuration are used as proton donors, then the photoswitching behavior of N\*-LCs induced by H-bonded chiral switches is detailedly investigated. We find that a helical inversion in the N\*-LCs, a phase transition from N\*-LCs to N-LCs, and the HTP increase or decrease in N\*-LCs could

be respectively achieved by just changing the length of terminal alkyl chain in proton donors upon light irradiation. Additionally, thermal switching behavior of N\*-LCs doped with H-bonded chiral switches is also demonstrated and the related mechanisms are addressed.

## Experimental Section

### Materials

In this study, all the chemicals and solvents were obtained from commercial sources and used without further purification. SLC1717 and 5CB were purchased from Shijiazhuang Chengzhi Yonghua Display Materials Co. Ltd (SLC1717: isotropic temperature,  $T_i = 92\text{ }^\circ\text{C}$ ;  $20\text{ }^\circ\text{C}$ , 589 nm,  $\Delta n = 0.201$ ; 5CB:  $T_i = 34\text{ }^\circ\text{C}$ ;  $20\text{ }^\circ\text{C}$ , 589 nm,  $\Delta n = 0.172$ ). All the crude products were purified by column chromatography, which was carried out on silica gel (200-300 mesh). Analytical thin layer chromatography (TLC) was performed on commercially coated 60 mesh GF254 glass plates.

### Synthesis of H-bonded proton acceptor

#### BNazo

**((S)-[1,1'-binaphthalene]-2,2'-diyl)bis(diazene-2,1-diyl)diphenol isonicotinate**

#### **(H-bonded proton acceptor):**

4,4'-((S)-[1,1'-binaphthalene]-2,2'-diyl)bis(diazene-2,1-diyl)diphenol was synthesized according to the procedure given in previous work.<sup>17,36</sup> And H-bonded proton acceptor, (S)-[1,1'-binaphthalene]-2,2'-diyl)bis(diazene-2,1-diyl)diphenol isonicotinate was further prepared following a procedure described in our previous study.<sup>37</sup>

$^1\text{H-NMR}$  (400MHz, Acetone):  $\delta$ = 8.88 (d,  $J$ =4.56Hz, 4H, N-H), 8.18 (d,  $J$ =9.2Hz, 2H, Ar-H), 8.11 (d,  $J$ =7.92Hz, 2H, Ar-H), 8.02 (t,  $J$ =4.68Hz, 4H, N-H), 7.57 (t,  $J$ =7.4Hz, 2H, Ar-H), 7.50 (d,  $J$ =8.36Hz, 2H, Ar-H), 7.42 (d,  $J$ =8.8Hz, 4H, Ar-H), 7.35 (m, 4H, Ar-H), 7.14 (d,  $J$ =8.76Hz, 4H, Ar-H).

IR (thin film)  $\nu_{\text{max}}$ : 2969, 1744, 1596, 1489, 1408, 1263, 1220, 1061 and  $749\text{cm}^{-1}$ .

### Synthesis of H-bonded proton donors

The H-bonded proton donors were synthesized starting from (R)-(+)-1,1'-bi-2-naphthol, as shown in Fig. 1. Their chemical structures were identified by FT-IR and  $^1\text{H NMR}$ .

#### I) (2'-Propoxy-1,1'-(R)-binaphthalen-2-yloxy)hexanoic acid ((R)-Proby)

To a solution of 1,1'-(R)-binaphthol (500 mg, 1.75 mmol) and  $\text{K}_2\text{CO}_3$  (300 mg, 2.18 mmol) in acetone (6 mL) was added dropwise, 1-Bromopropane (215 mg, 1.75 mmol). The resulting mixture was heated at reflux with stirring for 24 h before being filtered, collected the filtrate and evaporated under reduced pressure. And the residue was dissolved in anhydrous MeOH (5 mL). To this solution was added  $\text{K}_2\text{CO}_3$  (2.4 g, 17.4 mmol) and 6-bromohexanoic acid (1.02 g, 5.25 mmol). This mixture was heated at reflux for a further 24h before evaporation to dryness and dissolution in water (50 mL). The aqueous layer was then washed with diethyl ether (3\*30 mL) before acidification with 3 M HCl. The acidified solution was extracted with  $\text{CH}_2\text{Cl}_2$ , dried ( $\text{MgSO}_4$ ) before being evaporated under reduced pressure. The residue was purified by column chromatography on silica gel to obtain a yellow oil in a yield 30%.

$^1\text{H-NMR}$  (400 MHz, DMSO):  $\delta$ = 11.92 (s, H, -COOH), 8.03 (d,  $J$ =9.04 Hz, 2H, Ar-H), 7.93 (d,  $J$ =8.08 Hz, 2H, Ar-H), 7.56 (d,  $J$ =9.06 Hz, 2H, Ar-H), 7.31 (t,  $J$ =7.44 Hz, 2H,

Ar-H), 7.21 (t, J=6.95 Hz, 2H, Ar-H), 6.94 (t, J=8.52 Hz, 2H, Ar-H), 3.94 (m, 4H, -OCH<sub>2</sub>), 1.91 (m, 2H, -CH<sub>2</sub>-COOH), 1.52-0.82 (m, 8H, CH<sub>2</sub>), 0.52 (m, 3H, -CH<sub>3</sub>)

IR(thin film)  $\nu_{\max}$ : 3056, 2928, 2857, 1707, 1460, 1430, 1353, 1266, 1242, 1147, 1017 and 923 cm<sup>-1</sup>

Element analysis: calculated C(78.71), H(6.83), found C(78.51), H(6.979).

HRMS(-): calculated 442.21, found 442.2138.

### II) (2'-Hexyloxy-1,1'-(R)-binaphthalen-2-yloxy)hexanoic acid ((R)-Hexby)

<sup>1</sup>H-NMR (400 MHz, DMSO):  $\delta$ = 11.93 (s, H, -COOH), 8.03 (d, J=9.0 Hz, 2H, Ar-H), 7.93 (d, J=8.12 Hz, 2H, Ar-H), 7.56 (d, J=9.0 Hz, 2H, Ar-H), 7.31 (t, J=7.46 Hz, 2H, Ar-H), 7.20 (t, J=7.6 Hz, 2H, Ar-H), 6.95 (d, J=8.38 Hz, 2H, Ar-H), 3.96 (m, 4H, -OCH<sub>2</sub>), 1.93-1.89 (m, 2H, -CH<sub>2</sub>-COOH), 1.56-1.16 (m, 14H, CH<sub>2</sub>), 0.71-0.67 (m, 3H, -CH<sub>3</sub>).

IR(thin film)  $\nu_{\max}$ : 3056, 2928, 2857, 1707, 1460, 1430, 1353, 1266, 1241, 1147, 1016 and 926 cm<sup>-1</sup>.

Element analysis: calculated C(79.31), H(7.49), found C(79.20), H(7.633).

HRMS(-): calculated 484.26, found 484.2617.

### III) (2'-Heptoxy-1,1'-(R)-binaphthalen-2-yloxy)hexanoic acid ((R)-Hepby)

<sup>1</sup>H-NMR (400MHz, DMSO):  $\delta$ =11.91 (s, H, -COOH), 8.03 (d, J=9.04 Hz, 2H, Ar-H), 7.93 (d, J=8.12 Hz, 2H, Ar-H), 7.54 (d, J=9.06 Hz, 2H, Ar-H), 7.31 (t, J=7.46 Hz, 2H, Ar-H), 7.21 (t, J=7.59 Hz, 2H, Ar-H), 6.95 (t, J=8.34 Hz, 2H, Ar-H), 3.96 (m, 4H, -OCH<sub>2</sub>), 1.98 (m, 2H, -CH<sub>2</sub>-COOH), 1.23-0.86 (m, 16H, CH<sub>2</sub>), 0.8-0.76 (m, 3H, -CH<sub>3</sub>).

IR(thin film)  $\nu_{\max}$ : 3056, 2928, 2857, 1708, 1461, 1430, 1353, 1266, 1242, 1147, 1017 and 926 cm<sup>-1</sup>.

Element analysis: calculated C(79.49), H(7.68), found C(79.50), H(7.745).

HRMS(-): calculated 498.28, found 498.2775.

**IV) (2'-Octyloxy-1,1'-(R)-binaphthalen-2-yloxy)hexanoic acid ((R)-Otcby)**

<sup>1</sup>H-NMR (400MHz, DMSO):  $\delta$ = 11.92 (s, H, -COOH), 8.03 (d, J=9.0 Hz, 2H, Ar-H), 7.93 (d, J=8.2 Hz, 2H, Ar-H), 7.56 (d, J=8.96 Hz 2H, Ar-H), 7.31 (t, J=7.42Hz, 2H, Ar-H), 7.20 (t, J=7.24 Hz, 2H, Ar-H), 6.95 (d, J=8.34 Hz, 2H, Ar-H), 3.96 (m, 4H, -OCH<sub>2</sub>), 1.99 (m, 2H, -CH<sub>2</sub>-COOH), 1.38-1.09 (m, 18H, CH<sub>2</sub>), 0.84-0.81 (m, 3H, -CH<sub>3</sub>)

IR(thin film)  $\nu_{\max}$ : 3056, 2929, 2868, 1707, 1460, 1430, 1353, 1268, 1241, 1147, 1016 and 932 cm<sup>-1</sup>.

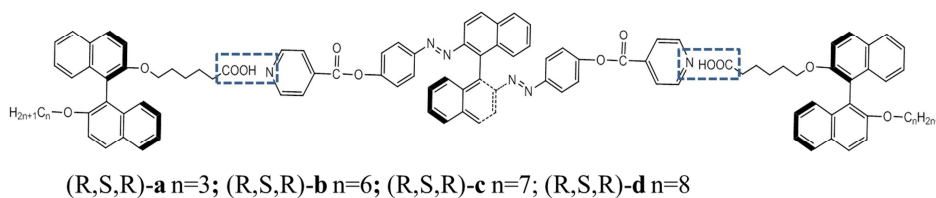
Element analysis: calculated C(79.65), H(7.86), found C(79.61), H(7.991).

HRMS(-): calculated 512.29, found 512.2935.

**Preparation of H-bonded chiral molecular switches**

H-bonded chiral switches were obtained by mixing the proton acceptor (BNAzo) with four proton donors ((R)-Proby, (R)-Hexby, (R)-Hepby and (R)-Octby) in molar ratio of 1:2 in THF respectively, and the mixture was stirred for 2 h at 60°C, followed by slow evaporation. Fig. 1 shows the chemical structures of these four H-bonded chiral switches (R,S,R)- **a**, **b**, **c**, **d**. Then we doped these H-bonded chiral switches with N-LCs hosts (SLC1717 and 5CB) to get N\*-LCs with self-organized helical superstructure.

### The chemical structures of the H-bonded chiral switches



### Synthesis of proton donors

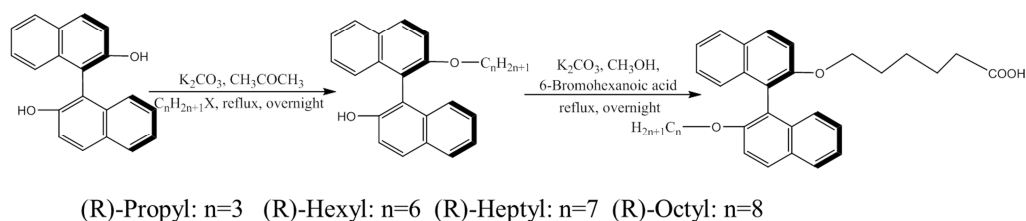


**Fig. 1** The chemical structures of the H-bonded chiral switches and synthetic route to the proton donors of the H-bonded chiral switches

### Measurements

We used FT-IR spectroscopy and variable-temperature FT-IR spectroscopy to confirm the self-assembly of H-bonded chiral switches. The FT-IR spectra were recorded on a Nicolet 5700 spectrometer at frequencies from 400 to 4000 cm<sup>-1</sup>. <sup>1</sup>H-NMR spectra were recorded at 400 MHz, on a German Bruker AV600 spectrometer. The pitches were determined by measuring the intervals of Cano's lines appearing on the surfaces of the wedge-type LC cells observed by a polarizing light microscope (POM, Leica DM2500P) with a hot stage calibrated with an accuracy of 0.1 °C (Linkam, THBS-600). The reflection spectra were examined with AvaSpec-2048 spectrophotometer in reflection mode. CD and UV-vis absorption spectra were recorded on a JASCO J810 spectrometer and a JASCO V550 spectrometer, respectively. UV irradiation experiments were carried out by mercury arc lamp

(Powerarc UV 100) through a filter at 365 nm.

## Results and Discussion

Here four H-bonded chiral switches (R,S,R)-**a**, **b**, **c**, **d** have been prepared by an uncomplicated self-assembly method. The chemical structures of them are presented in Fig. 1. As can be seen from the structural formulas, an axially chiral binaphthyl azobenzene with S configuration (*transoid* form,  $\theta > 90^\circ$ ) is selected as proton acceptor and two binaphthyl acids with R configuration (*transoid* form,  $\theta > 90^\circ$ ) are used as proton donor in these four H-bonded complexes. Here, it is worthy to note that the *transoid* form of (S)-binaphthyl in the proton acceptor induces a left-handed N\*-LCs, while the *transoid* form of (R)-binaphthyl in the proton donors leads to a right-handed N\*-LCs according to the experimental and previous theory.<sup>23</sup> The only difference in these four H-bonded complexes is the length of terminal flexible chain in binaphthyl acids. As a result, the terminal flexible chain greatly influences the initial HTP value of these four H-bonded chiral switches in N\*-LCs as mentioned later. Furthermore, the handedness induced by them in N\*-LCs could be decreased, neutralized, inverted or increased by changing the equilibrium of the chiral centers with the opposite chirality upon UV light irradiation. Additionally, the chiral induction also happens as the temperature changes due to the H-bonded effect and the change of dihedral angle induced by temperature. In this study, the photo- and thermo- switching behaviors of the N\*-LCs doped with the H-bonded chiral switches are investigated in detail, the molecular arrangements of N\*-LCs and the corresponding switching mechanisms are demonstrated in Fig. 2.

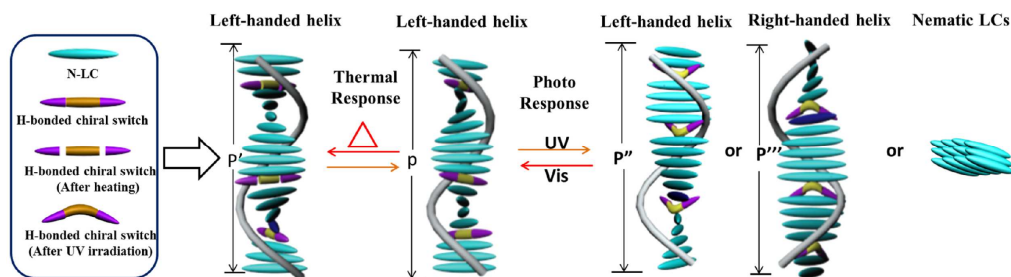


**Fig. 2** The schematic of the helical superstructure and the corresponding switching mechanism of H-bond chiral switches in N-LC hosts reversibly tuned by UV/Vis light and heat

First, FT-IR was used to verify the existence of hydrogen bond in H-bonded chiral switches. Two strong H-bond self-assembly processes could be found in our system, which include the  $-\text{OH}\dots\text{N}$  between proton donors and acceptors and the  $-\text{OH}\dots\text{O}=\text{C}-$  between carboxylic acid dimers. Fig. 3 shows the FT-IR spectra of the H-bonded chiral switches and their precursors. The formation of H-bond obtained by self-assembly process were confirmed by the FT-IR spectra. For example, two peaks at  $2533$  and  $1922\text{ cm}^{-1}$  indicate the presence of hydrogen bonds in H-bonded chiral switch ((R,S,R)-**a**) as shown in Fig. 3a, which coincides with the position of  $-\text{OH}$  stretching of H-bond between the carboxylic acid and pyridyl group.<sup>15,34</sup> Meanwhile, we find that the intensities of the peaks associated with carboxylic acid decrease in the Fig. 3a, this means that the H-bond between  $-\text{OH}\dots\text{N}$  have replaced the H-bond of  $-\text{OH}\dots\text{O}=\text{C}-$ . A similar trend could be observed in (R,S,R)-**b**, (R,S,R)-**c** and (R,S,R)-**d** as shown in Fig. 3b-d. These results demonstrate that four H-bonded chiral switches with different proton donors are successfully obtained.

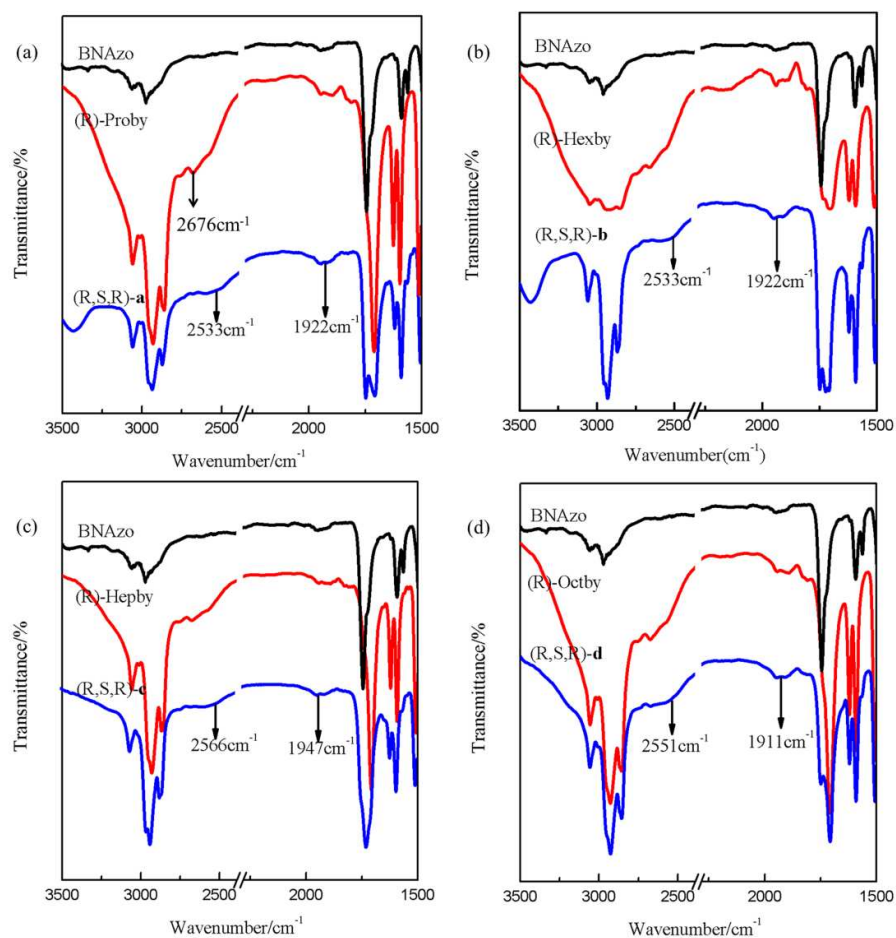


**Fig. 3** FT-IR spectra of the H-bonded spectra of the H-bonded chiral switches and their precursors (a): BNAzo, (R)-Proby, (R,S,R)-a; (b): BNAzo, (R)-Hexby, (R,S,R)-b; (c): BNAzo, (R)-Hepby, (R,S,R)-c; (d): BNAzo, (R)-Octby, (R,S,R)-d

Thermal stability of the H-bonded chiral switches was further investigated by means of variable-temperature FT-IR spectroscopy. As shown in Fig. 4a-d, we could observe two H-bonded characteristic peaks of all these H-bonded chiral switches at round 2500 and 1900  $\text{cm}^{-1}$  which results from the H-bonds between the carboxylic acid and pyridyl group as mentioned above. As the temperature increases from 20 to 180  $^{\circ}\text{C}$ , the intensities of these two peaks become gradually weak, which indicates that the H-bonds begin to rupture and H-bond interaction between the proton donor

and acceptor becomes weaker. Additionally, both Fig. S1 and the inset illustrations in Fig. 4a-d show that there also exists a slight reduction of these two peaks intensities in the temperature ranged from 20 to 80 °C. This modulation of the intermolecular forces between proton donor and acceptor with temperature has a positive contribution for the thermal sensitivity of N\*-LCs as mentioned later.

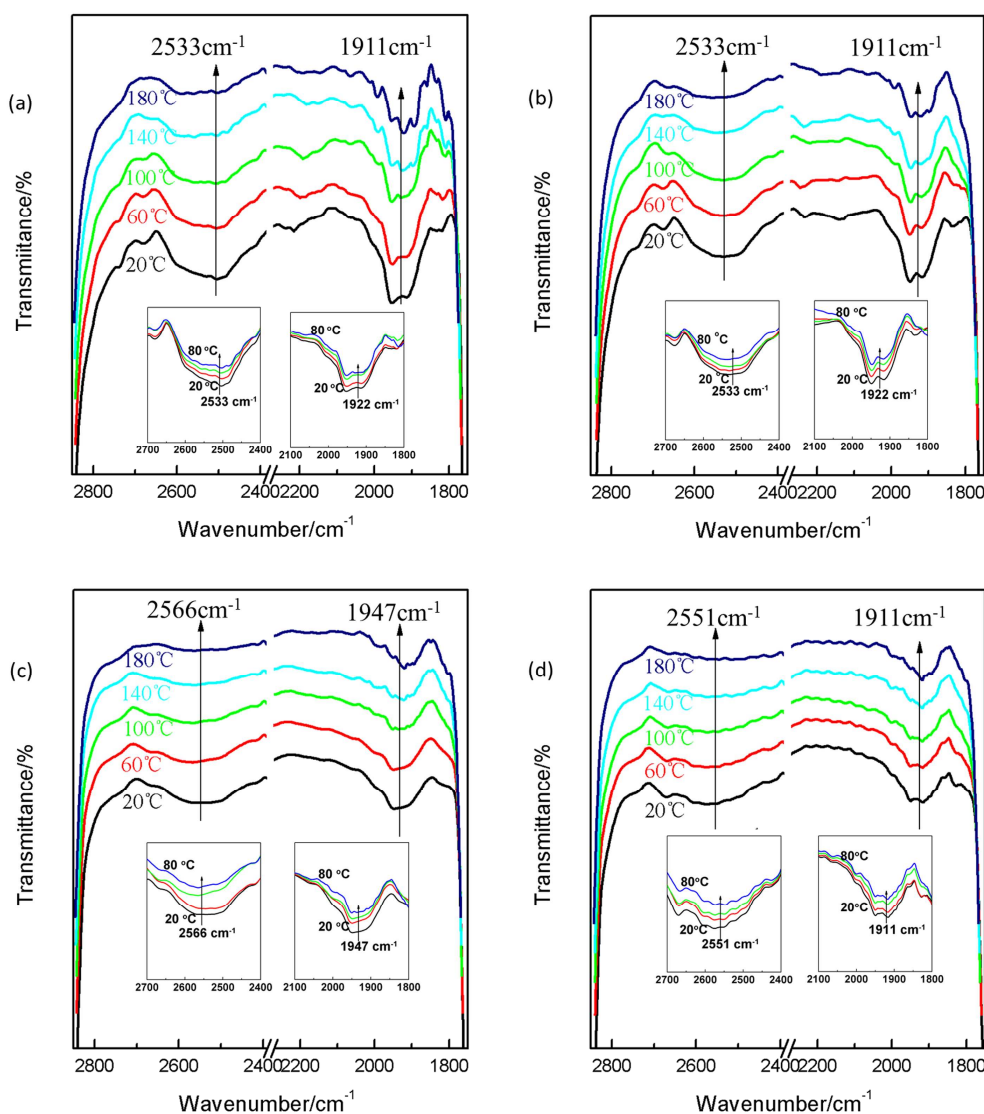


**Fig. 4** Variable-temperature FT-IR spectra of H-bonded chiral switches (a): (R,S,R)-**a**; (b): (R,S,R)-**b**; (c): (R,S,R)-**c**; (d): (R,S,R)-**d**

Photo-responsive behavior of these four H-bonded chiral switches in solution was

studied by using UV-vis spectroscopy and circular dichroism (CD) spectroscopy as shown in Fig. 5. By comparing the four H-bonded chiral switch ((R,S,R)-**a**, **b**, **c**, **d**) in both UV-vis spectra and CD spectra, we observe that the variation of the peak intensities exhibits a similar trend in the spectra. For example, (R,S,R)-**a** shows a typical azobenzene absorption spectrum with an intense  $\pi$ - $\pi^*$  transition at  $\lambda=350$  nm, and a weak  $n$ - $\pi^*$  transition near at  $\lambda=460$  nm in Fig. 5a. Upon UV photoirradiation at 365nm ( $2 \text{ mW}\cdot\text{cm}^{-2}$ ), a clear decrease in the  $\pi$ - $\pi^*$  band and a relatively small amount of increase in the  $n$ - $\pi^*$  band could be observed, this is because of the conformational switching of the azobenzene moieties from a *trans* to *cis* geometry of BNAzo unit in (R,S,R)-**a**. After around 80 s of UV light irradiation, the intensity no longer changes, demonstrating that the arrival of photostationary state (PSS365nm). Additionally, remarkable changes are also observed in the chiroptical properties as demonstrated in Fig. 5a, CD spectra also exhibit distinct bands for  $n$ - $\pi^*$  and  $\pi$ - $\pi^*$  transitions in (R,S,R)-**a**. At initial state, it shows a negative band and positive band for the  $\pi$ - $\pi^*$  transitions at 320 nm and 380 nm along with a relatively weak negative band at 450 nm. Then a gradual increase of the peak intensity at 450nm could be found after 365 nm UV irradiation at the intensity of  $2 \text{ mW}\cdot\text{cm}^{-2}$  due to the formation of *cis* isomer. Meanwhile the pattern of CD Cotton effect between 300 and 400 nm becomes weak due to the  $\pi$ - $\pi^*$  transitions, which is similar to the trend we observe in UV-vis spectra. Similar phenomena both in UV-vis spectra and CD are found in the case of (R,S,R)-**b**, **c**, **d** as shown in Fig. 5b-d, demonstrating these three switches also have *trans* state to *cis* state transformation upon UV irradiation.

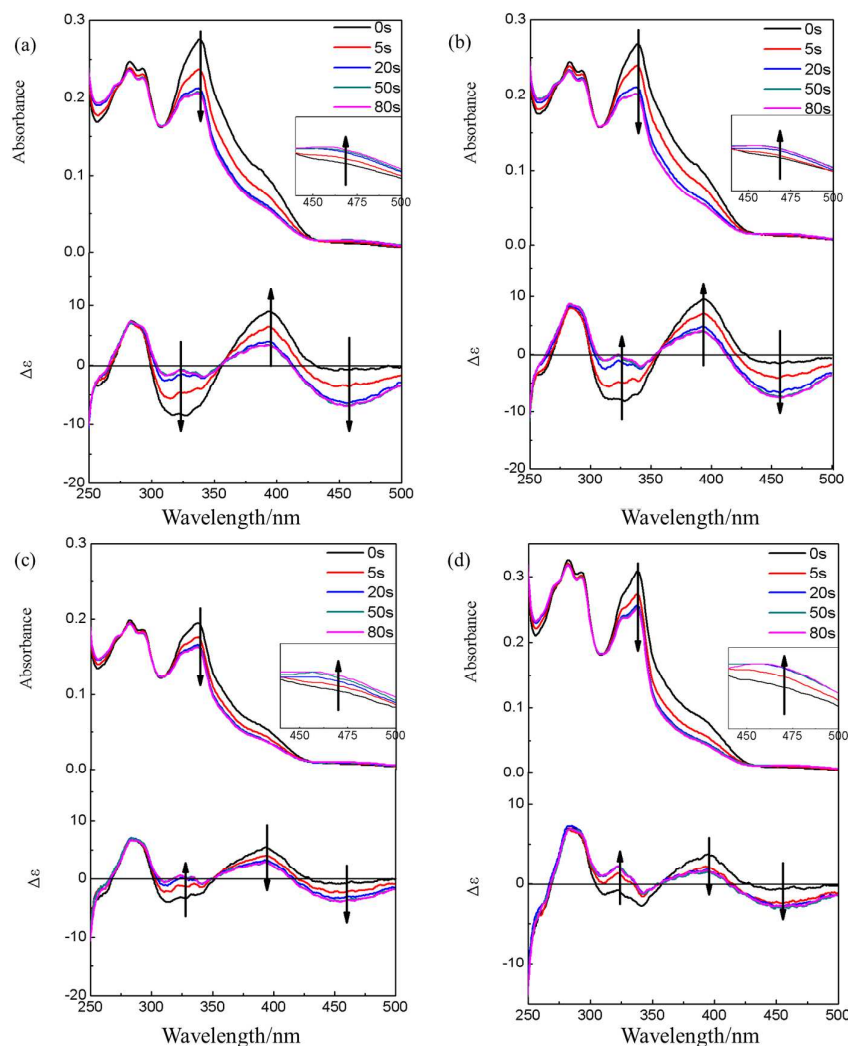


**Fig. 5** UV-Vis absorption and CD spectra of the H-bonded chiral switches in 1,4-dioxane under UV irradiation (a): (R,S,R)-**a**; (b): (R,S,R)-**b**; (c): (R,S,R)-**c**; (d): (R,S,R)-**d**

In order to evaluate the effectiveness of temperature on optical behavior of these four H-bonded chiral switches, we measured absorption spectra of (R,S,R)-**a**, **b**, **c**, **d** in 1,4-dioxane at various temperature. Herein, we note that the  $^1B_b$  band at 230 nm in Fig. 6 corresponds to a long axis of a naphthyl group, while  $^1L_a$  band at 290 nm corresponds to a short axis of it. As shown in Fig. 6, the absorbance intensities of the  $^1B_b$  band of the binaphthyl moiety decrease with increasing temperature. This change

is dependent on a dihedral angle between two naphthyl moieties as mentioned in the previous studies, and the change of  ${}^1B_b$  band further induces the molecular twisting of the binaphthyl moiety.<sup>38-40</sup> On the basis of these results of the thermal response behavior, we think that the raising and falling temperature may alter the dihedral angle of the binaphthyl moieties in these four chiral switches, thereby influencing the HTP values of the N\*-LCs induced by them.

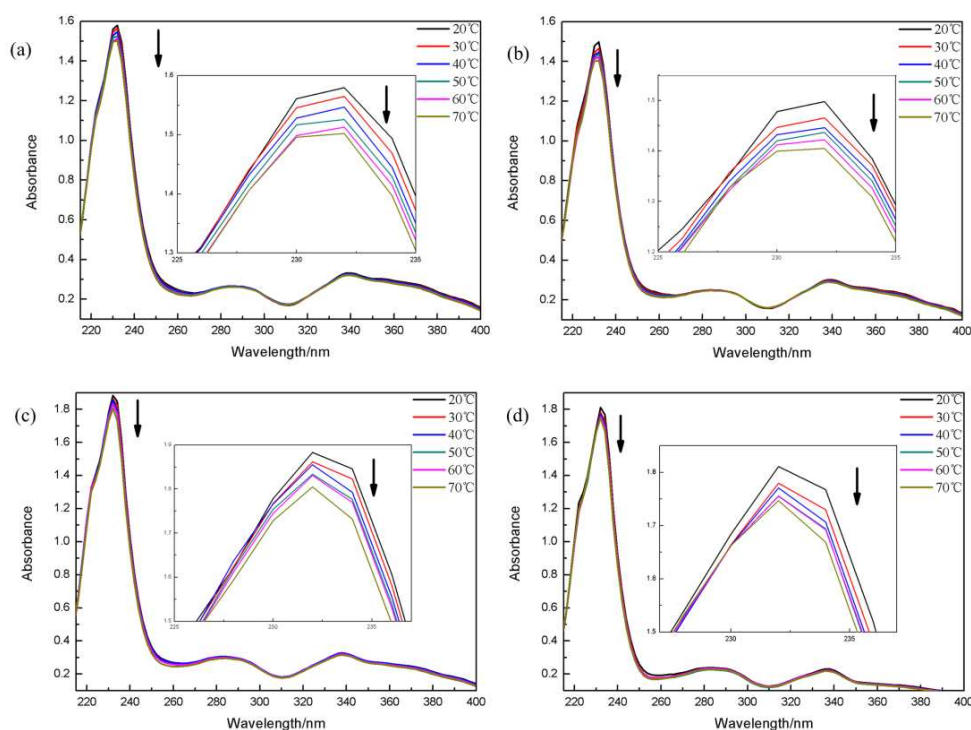


**Fig. 6** UV-Vis absorption spectra of the H-bonded chiral switches at various temperature (a): (R,S,R)-**a**; (b): (R,S,R)-**b**; (c): (R,S,R)-**c**; (d): (R,S,R)-**d**

To investigate the photo- and thermo-responsive behavior of N\*-LCs doped with H-bonded chiral switches, we prepared a series of N\*-LCs mixture by doping small amount of the (R,S,R)-**a**, **b**, **c**, **d** into two different nematic LC hosts (SLC1717 and 5CB), in which the weight ratios are corresponding to switch (R,S,R)-**a** : SLC1717 or 5CB host = 1:99 and switches (R,S,R)-**b**, **c**, **d** : SLC1717 or 5CB host = 3:97,

respectively. Here HTP value is used to estimate the ability of chiral dopant for twisting N\* mesophase and it is defined as the value of  $\beta$  and expressed by following equation:  $\beta=1/Pc$ , where P is the helical pitch and c is the concentration of the chiral dopant. Here, we employ a Cano's method in wedge cells to get the pitch values of these chiral switches and the pitch change as described in our previous study.<sup>15</sup>

It amazes us that the N\*-LCs samples with these four chiral switches exhibit distinct switching characteristics upon light irradiation. As shown in Fig. 7a, the distance between Cano lines of sample 1 with SLC-1717 and (R,S,R)-**a** increases after irradiation with UV light, which means the HTP value of (R,S,R)-**a** in N\*-LCs decreases because of *trans* to *cis* photoisomerization. In the case of sample 2 filled with 3 wt% (R,S,R)-**b** in SLC1717, the Cano lines move outward and disappear after 60 s upon irradiation with UV light at 365nm, and an apparent N phase is observed in the wedge cell as shown in Fig. 7b. We can further confirm the phase transition happens for the sample 2 in a homeotropic cell. The typical fingerprint texture of the N\* phase is clearly observed under POM at the initial state. Upon UV irradiation at 365 nm, the fingerprint texture disappeared and a transient N phase is confirmed with conoscopic observation as shown in Fig. 8a. Interestingly, in the case of sample 3 with 3 wt% (R,S,R)-**c** in SLC1717, we find the Cano lines disappear with UV irradiation at 365 nm for only 5s, and an apparent N phase is found in the wedge cell. Upon further UV irradiation, an oily streak texture gradually appears and the Cano lines form again at the  $PSS_{365nm}$  with 30 s as shown in Fig. 7c. As is well known that, handedness inversion occurs when the helix of one handedness unwinds, disappears at a certain

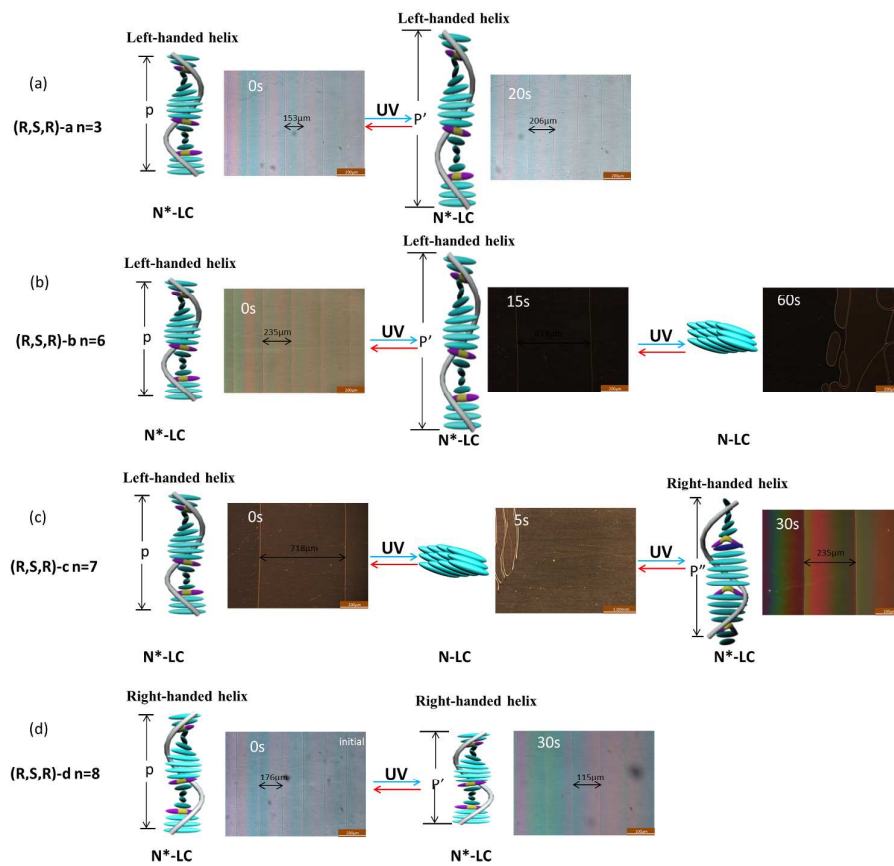


**Fig. 7** POM images of the wedge cell of photoresponsive N\*-LCs including (a): (R,S,R)-a (1.0 wt%), (b): (R,S,R)-b (3.0 wt%), (c): (R,S,R)-c (3.0 wt%), and (d): (R,S,R)-d (3.0 wt%), between the *trans* (left) and PSS (right) by irradiation of UV ( $\lambda = 365$  nm,  $2$  mW $\cdot$ cm $^{-2}$ ) at  $25$  °C. Along the corresponding POMs are described schematic illustrations of (a) only reversible HTP decreasing (b) reversible phase transition between N\*-LCs and N-LC and (c) reversible helical inversion between N\*-N-N\* phase transition sequence with opposite screw senses (d) only reversible HTP increasing upon UV light

point, and then forms a helix structure with the opposite handedness.<sup>21</sup> Therefore we confirm this N\*-N- N\* phase transition sequence is a direct evidence of the inversion of the N\* handedness in the sample 3. Meanwhile, we observe the same phase transition sequence in a homeotropic cell as shown in Fig. 8b. The typical fingerprint

texture of  $N^*$  phase under POM is observed at the initial stage. When the homeotropic cell is irradiation UV light at 365nm, the fingerprint texture disappears quickly and a transient  $N$  phase is confirmed with conoscopic observation. Continued UV irradiation results in the reappearance of the fingerprint texture, indicating the formation of another  $N^*$  phase with opposite handedness. Finally, as regards sample 4 with (R,S,R)-**d** and SLC-1717, the distance between Cano lines decreases in Fig. 7d after UV light irradiation, this suggests the HTP values of (R,S,R)-**d** increase in  $N^*$ -LCs.

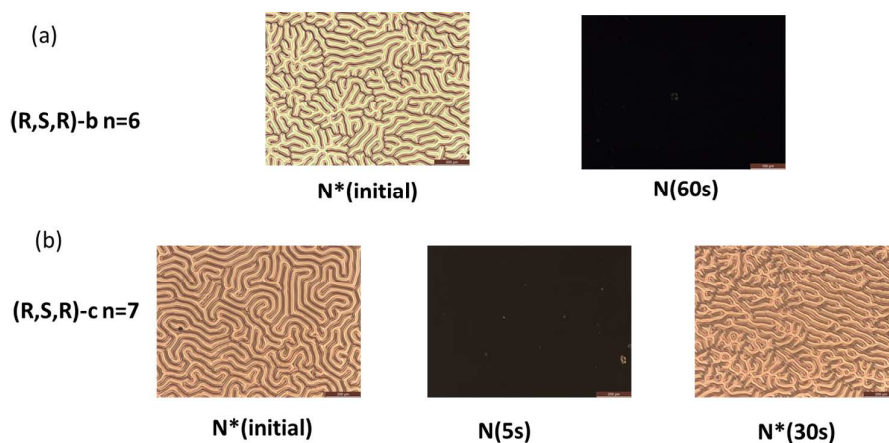


**Fig. 8** POMs images of the homeotropic cell of photoresponsive  $N^*$ -LCs including (a): (R,S,R)-**b**, and (b): (R,S,R)-**c** (3.0 wt%) between the *trans* (left) and PSS (right) by irradiation of UV ( $\lambda = 365$  nm,  $2 \text{ mW}\cdot\text{cm}^{-2}$ ) at  $25$  °C

Furthermore, HTPs of (R,S,R)-**a**, **b**, **c**, **d** in SLC1717 and 5CB hosts are calculated and summarized in Table 1. The results demonstrate that there is similar trend in HTP change of (R,S,R)-**a**, **b**, **c**, **d** both in SLC-1717 and 5CB. In Table 1, the positive sign and the negative sign represent right handedness and left handedness, respectively. It could be summed up as: Four different states including HTP decreases in  $N^*$ -LCs (LC

samples doped with (R,S,R)-**a**), a phase transition between the N\*-LCs and N-LCs (LC samples doped with (R,S,R)-**b**), a helical inversion in the N\*-LCs (LC samples doped with (R,S,R)-**c**) and HTP increases in N\*-LCs (LC samples doped with (R,S,R)-**d**) upon light irradiation could be achieved, respectively. This result may have several explanations. First, considering that overall HTP of H-bonded chiral switches is determined by both the proton acceptor of binaphthyl azobenzene and the proton donor of binaphthyl acids with opposite chiral configuration, we expect that the difference in HTPs between them will influence the overall helicity of the H-bonded chiral switches. Herein, as the length of terminal flexible chain in binaphthyl acids is increased, the HTP value of the proton donor with the right handedness increases. As a result, H-bonded chiral compounds (R,S,R)-**a**, **b**, **c**, **d** bearing with these two opposite chiral configurations are found to have a decreased initial HTP value. Second, Upon UV irradiation, the HTP value of the central proton acceptor decreases owing to the *trans-cis* isomerization upon UV light, while HTP values of the proton donors don't change. Therefore the conflicting chiralities and the shifting equilibrium between (S)-binaphthyl azobenzene and (R)-binaphthyl acids result in four different states. For example, a diagram schematic for this switching mechanism is provided as shown in Fig. 9. H-bonded chiral switch (R,S,R)-**c** induces a left-handed N\*-LCs in the initial state because the HTP value of the proton acceptor with the left handedness is bigger than that of the proton donors with the right handedness. Upon UV irradiation, H-bonded chiral switch (R,S,R)-**c** leads to a right-handed N\*-LCs in the photostable state, which is attributed to the decrease in HTP of the central proton

acceptor as mentioned above. Finally, by comparing of the HTP data in 5CB with that obtained in SLC-1717 in Table 1, we find that 5CB provide lower HTPs at the initial state, which might be due to the different interaction between H-bonded chiral switches and the host LCs. It should also be noted that all the above changes in these LC hosts are reversible by visible-light irradiation.

**Table 1.** Helical twisting power (in SLC1717 and 5CB) of H-bonded chiral switches at initial state and photostationary state upon UV irradiation (365nm, 2 mW·cm<sup>-2</sup>)<sup>[a]</sup>

H-bonded Chiral Molecular Switches	LC hosts	HTP (wt%)/ $\mu\text{m}^{-1}$		$\Delta\text{HTP}$ ( $\mu\text{m}^{-1}$ ) <sup>[b]</sup>	Change in HTP <sup>[c]</sup> (%)
		Initial	PSS <sub>UV</sub>		
(R,S,R)-a	SLC 1717	-12.48	-9.28	3.2	25.64
(R,S,R)-a	5CB	-8.64	-7.32	1.32	15.28
(R,S,R)-b	SLC1717	-2.78	--	2.78	--
(R,S,R)-b	5CB	-2.96	--	2.96	--
(R,S,R)-c	SLC1717	-0.89	+2.89	3.78	425
(R,S,R)-c	5CB	-0.39	+2.80	3.19	818
(R,S,R)-d	SLC1717	+3.49	+5.89	2.4	87.95
(R,S,R)-d	5CB	+1.80	+2.71	0.91	50.56

[a] Positive and negative signs represent right- and left-handed helical twists, respectively. [b]  $\Delta\text{HTP}$  is calculated by subtracting the photostationary HTP value from the initial HTP value. [c] The change in HTP is calculated by dividing  $\Delta\text{HTP}$  by initial HTP.

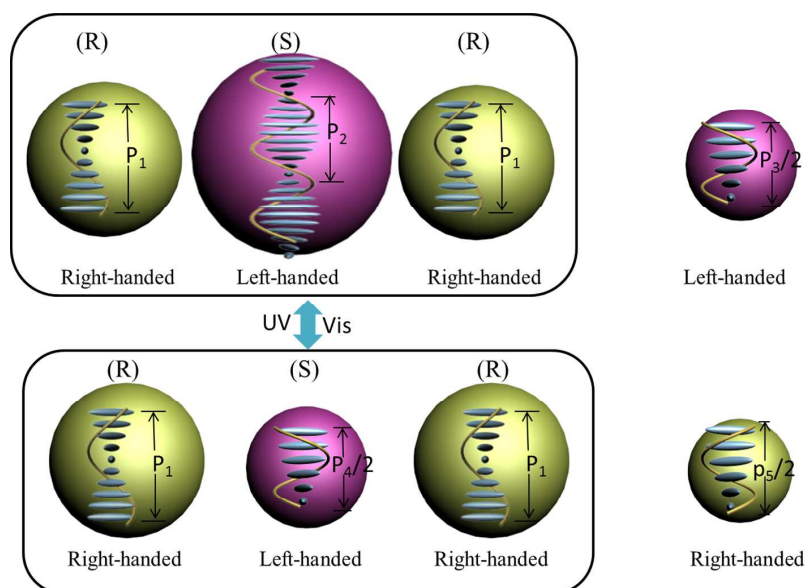
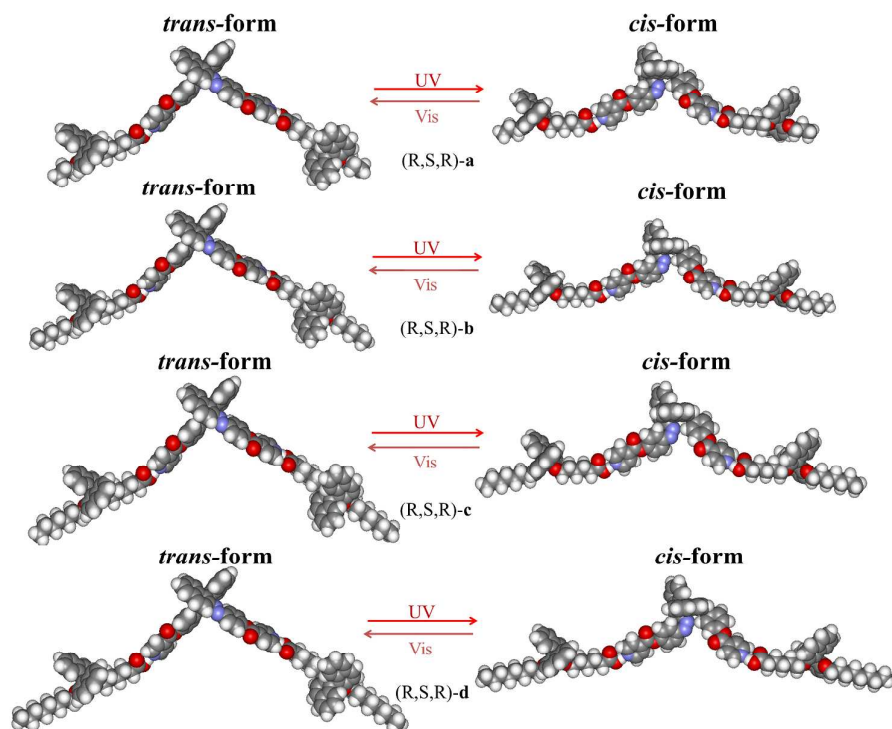


Fig. 9 Schematic illustration of the mechanism of handedness inversion in self-organized helical superstructures induced by H-bonded chiral switch

To gain further insight into the structure–property relationships, we evaluate the optimized geometries of the H-bonded chiral switch (R,S,R)-**a**, **b**, **c**, **d** by Gaussian 03 calculations at B3LYP/6-31G(d) level. We find that H-bonded chiral switch (R,S,R)-**a**, **b**, **c**, **d** have similar molecular conformations before and after UV irradiation, respectively. First, the central proton acceptor of the binaphthyl azobenzene in H-bonded chiral switch possesses rod shapes before UV irradiation in Fig. 10, while they are provided with bent shapes upon UV irradiation, which suggests that *trans-cis* photoisomerization takes place upon UV irradiation. Secondly, although the proton donors of binaphthyl acids in (R,S,R)-**a**, **b**, **c**, **d** have different terminal chain length, the molecular conformation of the central proton acceptor *is* not affected by them as shown in Fig. 10. What's more, the molecular conformations of the binaphthyl acids have no change before and after UV irradiation, which means that no changes of the proton donors happen during the *trans-cis* isomerization of the central proton acceptor upon UV irradiation.



**Fig. 10** Optimized structures of *trans* and *cis* form of (R,S,R)-**a**, (R,S,R)-**b**, (R,S,R)-**c** and (R,S,R)-**d** (space filling model) obtained by Gaussian 03 calculations at the B3LYP/6-31G(d) level.

The thermoresponsive behavior of N\*-LCs based on the H-bonded chiral switches is also studied by the Grandjean-Cano method. The changes of the pitch length are observed at various temperatures as shown in Fig. 11, and the inset images in Fig. 11 are the POM images of the samples in Cano wedge cells. It should also be noted that the variation of Cano lines length indicates the change of the pitch length of N\*-LCs and the corresponding HTP values of these H-bonded chiral switches as mentioned above. As shown in Fig. 11, it clearly shows that the pitch lengths of the N\*-LCs doped with (R,S,R)-**a** and (R,S,R)-**d** increase with increasing temperature, which means that the HTPs of (R,S,R)-**a** and (R,S,R)-**d** decrease with increasing temperature. While the pitch lengths of the N\*-LCs doped with (R,S,R)-**b** and (R,S,R)-**c** decrease

with increasing temperature, suggesting that the HTPs of (R,S,R)-**b** and (R,S,R)-**c** increase as the temperature is increased.

Let us discuss the reason why these four H-bonded chiral switches exhibit different thermal responsive behavior based on both effects of dihedral angle and H-bonded interaction. First, the dihedral angle of these four chiral switches changes with temperature (Fig. 6), which further affects the phase structure of the N\*-LCs. We find that the HTPs of both the proton donors and proton acceptor decrease with increasing temperature because of the changing of the dihedral angle of the binaphthyl groups (for details, see Figs. S2, S3 in Supporting Information, SI). Second, H-bonded interactions between the proton acceptor and the proton donors become weaker with temperature increasing according to the above real-time FT-IR data (Fig. 4). When the H-bonds become weak, we think that H-bonds in these four chiral switches begin to be partially ruptured with the temperature increasing. We unexpectedly find that the weakening or rupture of the H-bonds brings out the different changes of the HTPs. By comparing the measured the HTPs values of these four chiral H-bonded switches with the completely ruptured cases in LC systems (Fig. S4, SI), when we consider H-bonded effect as an only factor, it is reasonable to think that the pitch lengths in N\*-LCs increase and the corresponding HTPs of them decrease as the temperature increases in the case of (R,S,R)-**a** and (R,S,R)-**d**. However, the pitch lengths in N\*-LCs decrease and the corresponding HTPs of them increase with the temperature increasing in the case of (R,S,R)-**b** and (R,S,R)-**c**. Finally, based on these two factors, both the effects the dihedral angle and the H-bonded interaction lead to the HTPs

decrease with the increasing temperature in the cases of (R,S,R)-**a** and (R,S,R)-**d**. Nevertheless, these two factors have the opposite effect in the cases of (R,S,R)-**b** and (R,S,R)-**c**, and but the effect of H-bonded interaction plays a dominant role, thereby leading to the HTPs increase as the temperature rises. Consequently, this interpretation for both effects of dihedral angle and H-bonded interaction could well explain the present results that the HTPs of (R,S,R)-**a** and (R,S,R)-**d** decrease and the HTPs of (R,S,R)-**b** and (R,S,R)-**c** increase as the temperature increases. Our studies indicate that the different photo-/thermal switching behaviors of the N\*-LCs are enabled by controlling the length of the terminal flexible chain in H-bonded complexes. This allows us to adjust the initial HTP value of these four H-bonded chiral switches, so that the diversity of phase transition of the N\*-LCs has been achieved not only by UV/Vis light irradiation but also by the temperature variation.

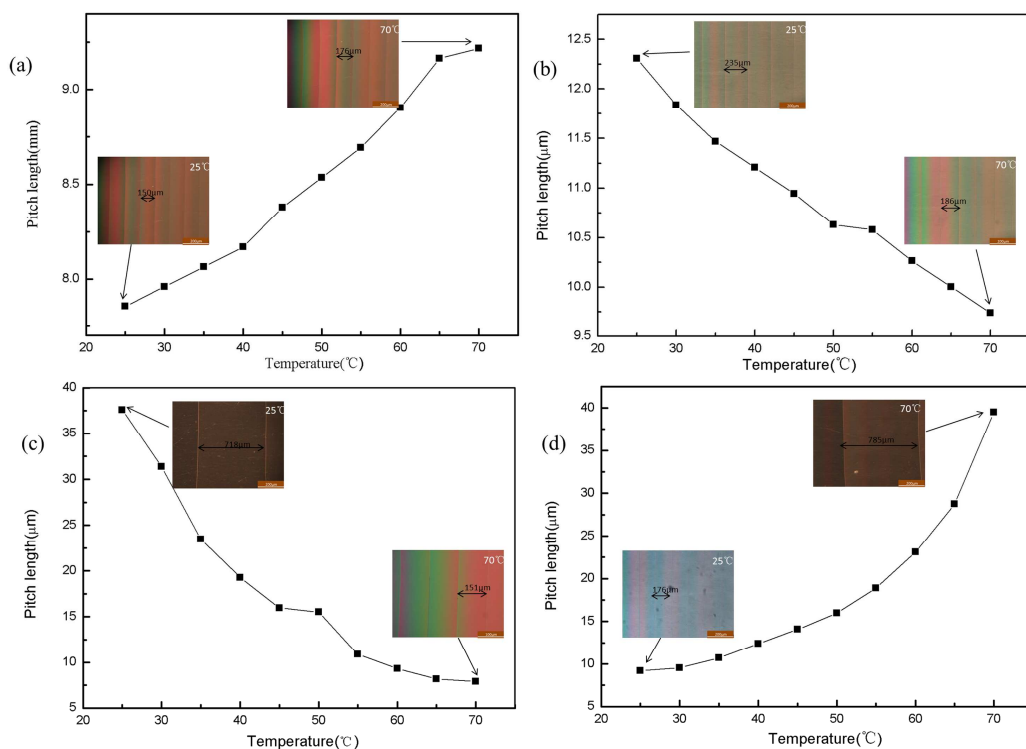


**Fig. 11** Changes in the helical pitch (a): (R,S,R)-**a** (1.0 wt%), (b): (R,S,R)-**b** (3.0 wt%), (c): (R,S,R)-**c** (3.0 wt%), and (d): (R,S,R)-**d** (3.0 wt%) in SLC1717 and POMs of Cano wedge cells at various temperatures

## Conclusions

In summary, we have developed a new kind of H-bonded chiral switches ((R,S,R)-**a**, **b**, **c**, **d**) by a facile self-assembly approach, in which binaphthyl azobenzene with the left handedness is used as the proton acceptor and binaphthyl acids with the right handedness are proton donors. Controlling the terminal flexible chain in binaphthyl acids of the proton donors leads to different initial HTP of (R,S,R)-**a**, **b**, **c**, **d**, thereby allowing for four conditions upon UV irradiation such as a helical inversion and a phase transition between N\*-LCs and N-LCs. The related switching mechanisms are due to the chiral counteraction and intensity attenuation of opposite chiral configurations between the proton acceptor and the proton donors during UV/Vis irradiation. Additionally, thermal switching behaviors of N\*-LCs based on H-bonded chiral switches are attributed to the modulation of the H-bonded interaction and the dihedral angles of the binaphthyl rings with temperature. We note that this simply strategy of the molecular design is of benefit us to understanding the structure–property relationships of the chiral molecules. Additionally, the H-bonding assembly method could provide new insights for developing responsive LC materials for photonics and display applications.

### **Acknowledgements**

This research was supported by the National Natural Science foundation (Grant no. 51373013 and 50903004) and Beijing Young Talents Plan (YETP0489). We also thank CHEMCLOUDCOMPUTING of Beijing University of Chemical Technology for the molecular simulation of this investigation.

## References

- 1 T. Muraoka, K. Kinbara and T. Aida, *Nature*, 2006, **440**, 512-515.
- 2 R. Eelkema, M. M. Pollard, N. Katsonis, J. Vicario, D. J. Broer and B. L. Feringa, *J. Am. Chem. Soc.*, 2006, **128**, 14397-14407.
- 3 M. Kawamoto, T. Aoki, N. Shiga and T. Wada, *Chem. Mater.*, 2009, **21**, 564-572.
- 4 M. Mathews and N. Tamaoki, *J. Am. Chem. Soc.*, 2008, **130**, 11409-11416.
- 5 Y. Wang and Q. Li, *Adv. Mater.*, 2012, **24**, 1926-1945.
- 6 P. C. R. Ballardini, A. Credi, M. T. Gandolfi, M. Maestri, M. Semararo, M. Venturi and V. Balzani, *Adv. Funct. Mater.*, 2007, **17**, 740-750.
- 7 Y. Xie, D. W. Fu, O. Y. Jin, H. Y. Zhang, J. Wei and J. B. Guo, *J. Mater. Chem. C.*, 2013, **1**, 7346-7356.
- 8 Y. L. Yu, M. Nakano and T. Ikeda, *Nature*, 2003, **425**, 145-145.
- 9 T. Muraoka, K. Kinbara and T. Aida, *Chem. Commun.*, 2007, 1441-1443.
- 10 T. Muraoka, K. Kinbara, Y. Kobayashi and T. Aida, *J. Am. Chem. Soc.*, 2003, **125**, 5612-5613.
- 11 H. Bisoyi and Q. Li, *Acc. Chem. Res.*, 2014, **47**, 3184-3195.
- 12 Y. Kim and N. Tamaoki, *J. Mater. Chem. C.*, 2014, **2**, 93258-9264.
- 13 Chilaya, G. (2001). Springer series partially ordered systems. In: H. Kitzerow & C. Bahr (Eds.), *Chirality in Liquid Crystals*, Springer: New York, pp. 28-67.
- 14 T. J. White, M. E. McConney and T. J. Bunning, *J. Mater. Chem.*, 2010, **20**, 9832-9847.
- 15 F. J. Chen, J. B. Guo, Z. J. Qu and J. Wei, *J. Mater. Chem.*, 2011, **21**, 8574-8582.

- 16 D. J. Mulder, A. P. H. J. Schenning and C. W. M. Bastiaansen, *J. Mater. Chem. C.*, 2014, **2**, 6695-6705.
- 17 O. Y. Jin, D. W. Fu, Y. X. Ge, J. Wei and J. B. Guo, *New J. Chem.*, 2015, **39**, 254-261.
- 18 K. Kishikawa, S. Aoyagi, M. Kohri, T. Taniguchi, M. Takahashi, S. Kohmoto, *Soft Matter*, 2014, **10**, 6582-6588.
- 19 Y. Han, K. Pacheco, C. W. M. Bastiaansen, D. J. Broer, R. P. Sijbesma, *J. Am. Chem. Soc.*, 2010, **132**, 2961-2967.
- 20 J. B. Guo, H. Wu, L. P. Zhang, W. L. He, H. Yang and J. Wei, *J. Mater. Chem.*, 2010, **20**: 4094-4102.
- 21 R. A. van Delden, T. Mecca, C. Rosini and B. L. Feringa, *Chem. Eur. J.*, 2004, **10**, 61-70.
- 22 M. Mathews and N. Tamaoki, *Chem. Commun.*, 2009, 3609-3611.
- 23 Y. Li, C. Xue, M. Wang, A. Urbas and Q. Li, *Angew. Chem. Int. Edit.*, 2013, **52**, 13703-13707.
- 24 H. Hayasaka, T. Miyashita, M. Nakayama, K. Kuwada and K. Akagi, *J. Am. Chem. Soc.*, 2012, **134**, 3758-3765.
- 25 M. Mathews, R. S. Zola, S. Hurley, D. K. Yang, T. J. White, T. J. Bunning and Q. Li, *J. Am. Chem. Soc.*, 2010, **132**, 18361-18366.
- 26 Y. Li, M. Wang, T. J. White, T. J. Bunning and Q. Li, *Angew. Chem. Int. Edit.*, 2013, **52**, 8925-8929.
- 27 M. Mitov and N. Dessaud, *Nat. Mater.*, 2006, **5**, 361-364.

- 28 J. B. Guo, H. Cao, J. Wei, D. Zhang, F. Liu, G. Pan, D. Zhao, W. He and H. Yang, *Appl. Phys. Lett.*, 2008, **93**, 201901(1)-(3).
- 29 M. H. Song, B. Park, K. C. Shin, T. Ohta, Y. Tsunoda, H. Hoshi, Y. Takanishi, K. Ishikawa, J. Watanabe, S. Nishimura, T. Toyooka, Z. Zhu, T. M. Swager and H. Takezoe, *Adv. Mater.*, 2004, **16**, 779-783.
- 30 M. Mitov, *Adv. Mater.*, 2012, **24**, 6260-6276.
- 31 M. E. McConney, V. P. Tondiglia, J. M. Hurtubise, T. J. White and T. J. Bunning, *Chem. Commun.*, 2011, **47**, 505-507.
- 32 J. B. Guo, F. J. Chen, Z. J. Qu, H. Yang and J. Wei, *J. Phys. Chem. B*, 2011, **115(5)**, 861-868.
- 33 D. J. Broer, C. M. W. Bastiaansen, M. G. Debije, and A. P. H. J. Schenning, *Angew. Chem. Int. Ed.*, 2012, **51**, 7102-7109.
- 34 Y. Shi, X. W. Wang, J. Wei, H. Yang and J. B. Guo, *Soft Matter*, 2013, **9**, 10186-10195.
- 35 F. J. Chen, J. B. Guo, O. Y. Jin and J. Wei, *Chin. J. Polym. Sci.*, 2013, **31**, 630-640.
- 36 S. Pieraccini, S. Masiero, G. P. Spada and G. Gottarelli, *Chem. Commun.*, 2003, 598-599.
- 37 O. Y. Jin, D. W. Fu, J. Wei, H. Yang and J. B. Guo, *RSC Adv.*, 2014, **4**, 28597-28600.
- 38 L. Di Bari, G. Pescitelli and P. Salvadori, *J. Am. Chem. Soc.*, 1999, **121**, 7998-8004.
- 39 L. Di Bari, G. Pescitelli, F. Marchetti and P. Salvadori, *J. Am. Chem. Soc.*, 2000,

122, 6395-6398.

40 M. Kawamoto, T. Aoki and T. Wada, *Chem. Commun.*, 2007, 930-932.

Graphic Abstract:

## Table of contents entry

**Text:**

The Effect of terminal chain length in hydrogen-bonded chiral switches on photo- and thermo- switching behavior of chiral nematic liquid crystals has been demonstrated.

**Color graphic:**

